J. Phase Equilib. Diffus. (2018) 39:702–713
https://doi.org/10.1007/s11669-018-0675-7

Experimental Diffusion Research on BCC Ti-Mn Binary and Ti-Al-Mn Ternary Alloys

Xiang Huang[1] · Junyi Tan[1] · Yanhua Guo[1] · Guanglong Xu[1] · Yuwen Cui[1,2]

Submitted: 25 May 2018 / in revised form: 13 June 2018 / Published online: 31 August 2018

Abstract Interdiffusion in the BCC phase of the Ti-Mn binary and Ti-Al-Mn ternary systems was investigated between 1273 and 1473 K by applying the diffusion-couple technique. The local chemical compositions within the interdiffusion zone of the diffusion couples were acquired by electron probe microanalysis (EPMA). The raw composition profiles were then analytically represented by the error function expansion, which allow the ternary inter- and impurity diffusivities to be appropriately extracted by the Whittle–Green and generalized Hall methods, respectively. It was demonstrated that, all four diffusion coefficients $\tilde{D}_{ij}^{k}$ (i, j = Al, Mn), both main and cross ones, increase with increasing the composition of diffusing specie at 1473 K, whereas at 1273 K $\tilde{D}_{\mathrm{MnMn}}^{\mathrm{Ti}}$ and $\tilde{D}_{\mathrm{MnAl}}^{\mathrm{Ti}}$ are enhanced by the addition of diffusing specie Mn but $\tilde{D}_{\mathrm{AlAl}}^{\mathrm{Ti}}$ and $\tilde{D}_{\mathrm{AlMn}}^{\mathrm{Ti}}$ are in weak dependence with the Al content. A complete comparison among seven Ti-Al-X (Ni, Co, Fe, Mn, Cr, V and Mo) ternary systems reveals that the order of the average main interdiffusion coefficients $\overline{\tilde{D}_{\mathrm{XX}}^{\mathrm{Ti}}}$ (X = Ni, Co, Fe, Mn, Cr, V and Mo) exhibits $D_{\mathrm{Ni}} > D_{\mathrm{Co}} > D_{\mathrm{Fe}} > D_{\mathrm{Mn}} > D_{\mathrm{Cr}} > D_{\mathrm{V}} > D_{\mathrm{Mo}}$.

Keywords BCC phase · generalized Hall method · impurity diffusivity · interdiffusion · Ti-Al-Mn ternary · Ti-Mn binary · Whittle–Green method

1 Introduction

Titanium alloys have high specific strength, considerable ductility and extraordinary corrosion resistance and good crack propagation resistance. These properties boost the widespread application of titanium alloys in aerospace, chemical and medical industries chemistry[1] as well as astro vehicle.[2] The performance of high-strength Ti alloys is governed by the combination of many factors, particularly including chemical compositions, grain size, precipitation, morphology of α (i.e. HCP) and β (i.e. BCC) phases, texture, etc. These processes are largely ascribed to diffusional transformation(s) during thermo-mechanical processing that ultimately lead to the development of "good" microstructure.

The conventional high-strength Ti alloys contain β-stabilizing elements of Cr, V, Nb, Mo, Fe and Mn, which, in addition to strengthening the BCC phase, can greatly enhance the fabricability or ductility of alloys during both hot and cold working operations, and confer a larger heat treatment capability or processing window.[3] While superplastic deformation behavior of Ti-Al-Mn near-α titanium alloys has been recently studied for superplastic forming as complex shape aerospace components,[4] Sumi et al.[5] studied the influence of Mn contents from 8 to 12% in BCC Ti-3%Al-1%Fe alloys

This invited article is part of a special issue of the *Journal of Phase Equilibria and Diffusion* in honor of Prof. Zhanpeng Jin's 80th birthday. The special issue was organized by Prof. Ji-Cheng (JC) Zhao, The Ohio State University; Dr. Qing Chen, Thermo-Calc Software AB; and Prof. Yong Du, Central South University.

✉ Yanhua Guo
guoyanhua@njtech.edu.cn

✉ Yuwen Cui
ycui@unizar.es

[1] Tech Institute for Advanced Materials and School of Materials Science and Engineering, Nanjing Tech University, Nanjing 210009, People's Republic of China

[2] ICMA Instituto de Ciencia de Materiales de Aragón, 50009 Saragossa, Spain

(mass%) on mechanical properties after solution heat treatment. They found that the ductility and toughness increased with increasing the Mn content up to 10%, accompanied with the dissolution of the α-stabilizing element Al into the BCC lattice up to about 5 wt.%, serving as indispensable component in high strength titanium alloys. Lu et al.[6] concluded that the addition of Al could increase the melting point, obtain the required percentage of α platelets for strengthening or developing bimodal microstructures for fatigue property improvement, and lessen the reactivity of titanium, thus facilitating the casting process.

So far, impurity and interdiffusivities in the Ti-based BCC solid solutions have been extensively measured in many binaries[7–11] and ternaries (e.g. Ti-Al-Co,[12] Ti-Al-Fe,[13] Ti-Al-Ni,[14] Ti-Al-Mo.[15]). Santos et al.[16] measured the tracer diffusivities of Ti^{44} and Mn^{54} in BCC Ti-Mn alloys ranging from 1073 to 1573 K, whereas Nakamura et al.[17] determined the impurity diffusion of Mn^{54} in single crystal HCP-Ti from 878 to 1135 K. To the best knowledge of authors, the interdiffusion coefficients of BCC Ti-Mn binary and Ti-Al-Mn ternary systems remain unknown. Therefore, the efforts are made in the present work to measure the inter- and impurity diffusion coefficients of the BCC Ti-Mn and Ti-Al-Mn alloys between 1273 and 1473 K by using the solid-state diffusion couple technique. By a way of comparison, the measured diffusion data will be then deduced to depict the diffusion characteristics of BCC Ti-Al-Mn alloys.

2 Materials and Methods

2.1 Experimental Procedure

Sixteen binary and four ternary Ti-based alloys in Table 1, with their nominal compositions placed in the BCC solid solution region according to the accepted phase diagrams[18] were prepared from 99.99 wt.% sponge Ti, 99.99 wt.% Al and 99.9 wt.% Mn by induction melting in an argon atmosphere. The melting was repeated five times to attain a homogeneous composition. The ingots were then solid-solutioned at 1473 K for 8 h under vacuum followed by water quenching that resulted in the homogeneous alloys with average grain size larger than several millimeters such that the effect of grain boundary diffusion can be neglected. The actual chemical compositions of the homogenized ingots were given by averaging several raw EPMA values and are listed in Table 1.

Small disk samples with the size of 10 × 10 × 5 (mm) were cut from the ingots by using wire-electrode cutting. Small disks were then prepared by polishing one top surface of the cylinder samples and annealed pure Ti to mirror-like quality. The well-contacted diffusion couples were assembled with appropriate pairs of the small disks by diffusion-bonding under vacuum at 1173 K for 4 h under a load with a stainless-steel clamp set. Tantalum foils were placed to separate the diffusion couple and clamps so that direct contact, thus possible contamination, between them could be avoided. The diffusion couples were sealed into evacuated and argon-back-flushed quartz capsules, and finally were subjected to interdiffusion annealing at predesigned condition (refer to Table 2 for annealing temperatures and times) followed by quenching in ice water. As listed in Table 2, five groups of binary diffusion couples (i.e. C1–C5) and eighteen groups of ternary diffusion couples (i.e. A1–A9 and B1–B9) were successfully fabricated that underwent various diffusion annealing. The diffusion couples were then sectioned parallel to the diffusion direction which suffered no oxidation and evaporation of elements, mounted, and polished by standard metallographic techniques. The microstructure of diffusion zone was observed by scanning electron microscopy (SEM) and the local composition was analyzed by electron microprobe analysis (EPMA) on JEOL JXA 8900.

Table 1 Terminal compositions of Ti-Mn and Ti-Al-Mn ingots (at.%)

Ingots	Nominal composition, at.%	Actual composition, at.%
T1	Ti-3Al	Ti-2.76Al
T2	Ti-5Al	Ti-4.87Al
T3	Ti-6Al	Ti-5.77Al
T4	Ti-8Al	Ti-7.81Al
T5	Ti-10Al	Ti-9.86Al
T6	Ti-15Al	Ti-14.09Al
T7	Ti-20Al	Ti-19.15Al
M1	Ti-5Mn	Ti-4.47Mn
M2	Ti-7Mn	Ti-6.76Mn
M3	Ti-10Mn	Ti-10.03Mn
M4	Ti-14Mn	Ti-13.86Mn
M5	Ti-22Mn	Ti-20.24Mn
M6	Ti-22Mn	Ti-18.12Mn
M7	Ti-22Mn	Ti-25.93Mn
M8	Ti-22Mn	Ti-17.46Mn
M9	Ti-22Mn	Ti-21.81Mn
TAM1	Ti-6Al-15Mn	Ti-5.87Al-14.65Mn
TAM2	Ti-10Al-10Mn	Ti-9.53Al-9.99Mn
TAM3	Ti-10Al-17Mn	Ti-9.68Al-15.09Mn
TAM4	Ti-20Al-10Mn	Ti-19.23Al-9.67Mn

2.2 Extraction of Diffusion Coefficients

The error function expansion (ERFEX)[14, 15, 19] was applied to analytically fit and represent the composition profiles acquired from the EPMA, allowing to eliminate the

Table 2 Assembly of diffusion couples

Diffusion couple	1st half	2nd half	Temperature, K	Annealing time, h
C1	Pure Ti	M5	1273	28
C2	Pure Ti	M6	1323	23
C3	Pure Ti	M7	1373	24
C4	Pure Ti	M8	1423	18
C5	Pure Ti	M9	1473	12
A1	T1	M1	1273	50
A2	T1	M3	1273	50
A3	T3	M3	1273	50
A4	T3	M4	1273	50
A5	T4	M4	1273	50
A6	T4	M9	1273	50
A7	Pure Ti	TAM1	1273	50
A8	Pure Ti	TAM2	1273	50
A9	T1	TAM2	1273	50
B1	T2	M2	1473	12
B2	T2	M4	1473	12
B3	T5	M4	1473	12
B4	T6	M4	1473	12
B5	T6	M5	1473	12
B6	T7	M5	1473	12
B7	Pure Ti	TAM3	1473	12
B8	Pure Ti	TAM4	1473	12
B9	T5	TAM4	1473	12

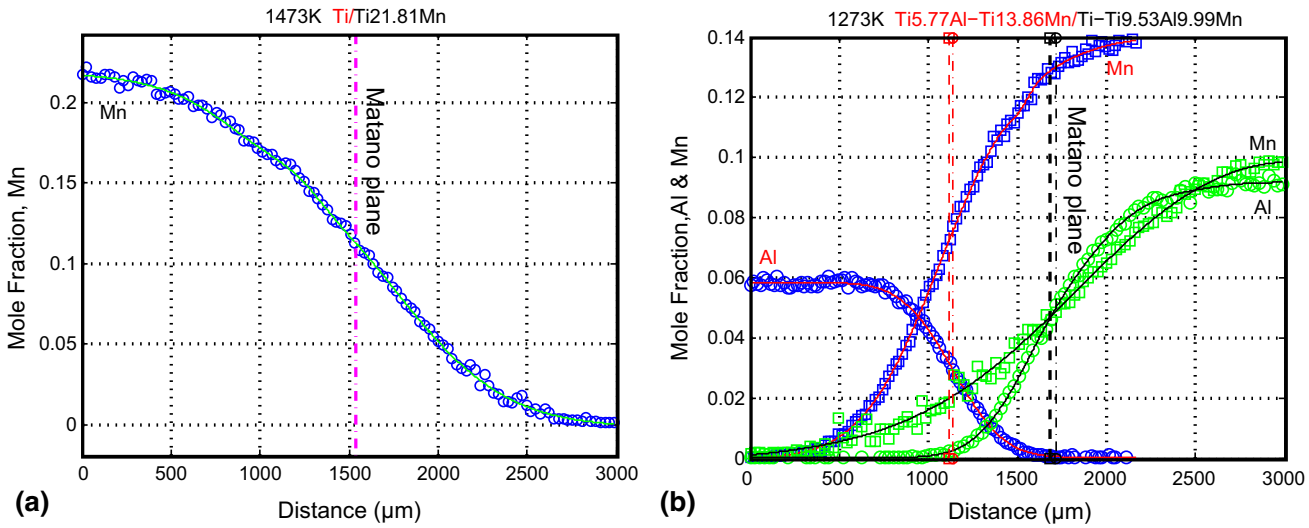

Fig. 1 Composition profiles of Ti-Mn and Ti-Al-Mn couples. (a) C5 at 1473 K for 12 h, (b) A4 and A8 at 1273 K for 12 h. The symbols are EPMA data, and the curves are the analytical ERFEX forms

local point-to-point fluctuations and the inaccuracy associated with the asymmetrical profiles. The expression of ERFEX is

$$x(z) = \sum_i a_i \mathrm{erf}[(b_i - c_i)z + d_i] \qquad \text{(Eq 1)}$$

where $x(z)$ is the represented composition at the diffusion distance z, a_i, b_i, c_i and d_i (i is typically up to 4) are the fitting parameters. The ERFEX physically enables the slope at the ends of the composition profile to be zero, as shown in Fig. 1, and it ensures that the impurity diffusivity of third element in binary alloys is extracted in a physical sense.

The Sauer–Freise (*S–F*)[20] and Whittle–Green (*W–G*)[21] methods were employed respectively to extract the interdiffusion coefficients of Ti-Mn binary and Ti-Al-Mn ternary BCC alloys from the ERFEX-processed profiles. Compared with the conventional Boltzmann–Matano method[22] in binary and Matano–Kirkaldy (*M–K*) method[23] in ternary, the *S–F* and *W–G* methods allow to extract the interdiffusion coefficients from diffusion profiles more accurately without suffering from the error of positioning the Matano plane.[22, 24]

In the *S–F* and *W–G* methods, a normalized composition variable $Y = \frac{x-x_L}{x_R-x_L}$ is introduced, where x_L and x_R represent the compositions at the far left and far right ends, respectively.[21, 25] The expression of binary interdiffusion coefficient yields Eq 2,

$$\tilde{D}(Y^*) = \frac{V_m}{2t(dY/dz)_{Z^*}}\left[(1-Y^*)\int_{-\infty}^{Z^*}\frac{Y}{V_m}dz + Y^*\int_{Z^*}^{+\infty}\frac{1-Y}{V_m}dz\right] \quad \text{(Eq 2)}$$

where V_m is the molar volume and t is the diffusion time, while the ternary interdiffusion terms of Ti-Al-Mn ternary can be derived by Eq 3a and 3b

$$\frac{1}{2t}\left(\frac{\partial z}{\partial Y_{\mathrm{Al}}}\right)_{Z*}\left[(1-Y_{\mathrm{Al}})\int_{-\infty}^{Z*}Y_{Al}dz + Y_{\mathrm{Al}}\int_{Z*}^{+\infty}(1-Y_{\mathrm{Al}})dz\right] = \tilde{D}^{\mathrm{Ti}}_{\mathrm{AlAl}} + \tilde{D}^{\mathrm{Ti}}_{\mathrm{AlMn}}\frac{\partial x_{\mathrm{Mn}}}{\partial x_{\mathrm{Al}}} \quad \text{(Eq 3a)}$$

$$\frac{1}{2t}\left(\frac{\partial z}{\partial Y_{\mathrm{Mn}}}\right)_{Z*}\left[(1-Y_{\mathrm{Mn}})\int_{-\infty}^{Z*}Y_{\mathrm{Mn}}dz + Y_{\mathrm{Mn}}\int_{Z*}^{+\infty}(1-Y_{\mathrm{Mn}})dz\right] = \tilde{D}^{\mathrm{Ti}}_{\mathrm{MnMn}} + \tilde{D}^{\mathrm{Ti}}_{\mathrm{MnAl}}\frac{\partial x_{\mathrm{Al}}}{\partial x_{\mathrm{Mn}}} \quad \text{(Eq 3b)}$$

where $\tilde{D}^{\mathrm{Ti}}_{\mathrm{AlAl}}$ and $\tilde{D}^{\mathrm{Ti}}_{\mathrm{MnMn}}$ are the main or direct ternary interdiffusion coefficients, $\tilde{D}^{\mathrm{Ti}}_{\mathrm{AlMn}}$ and $\tilde{D}^{\mathrm{Ti}}_{\mathrm{MnAl}}$ are the cross or indirect ones. All four interdiffusion coefficients can be determined by solving Eq 3a and 3b simultaneously from

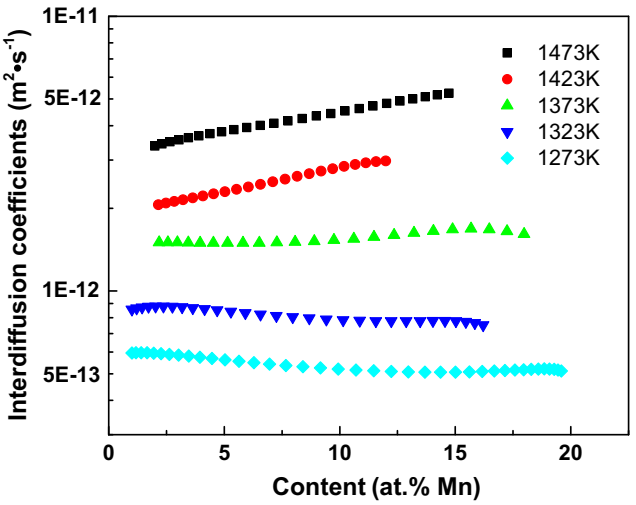

Fig. 3 Interdiffusion coefficients of BCC Ti-Mn binary alloys in Ti-Mn binary system

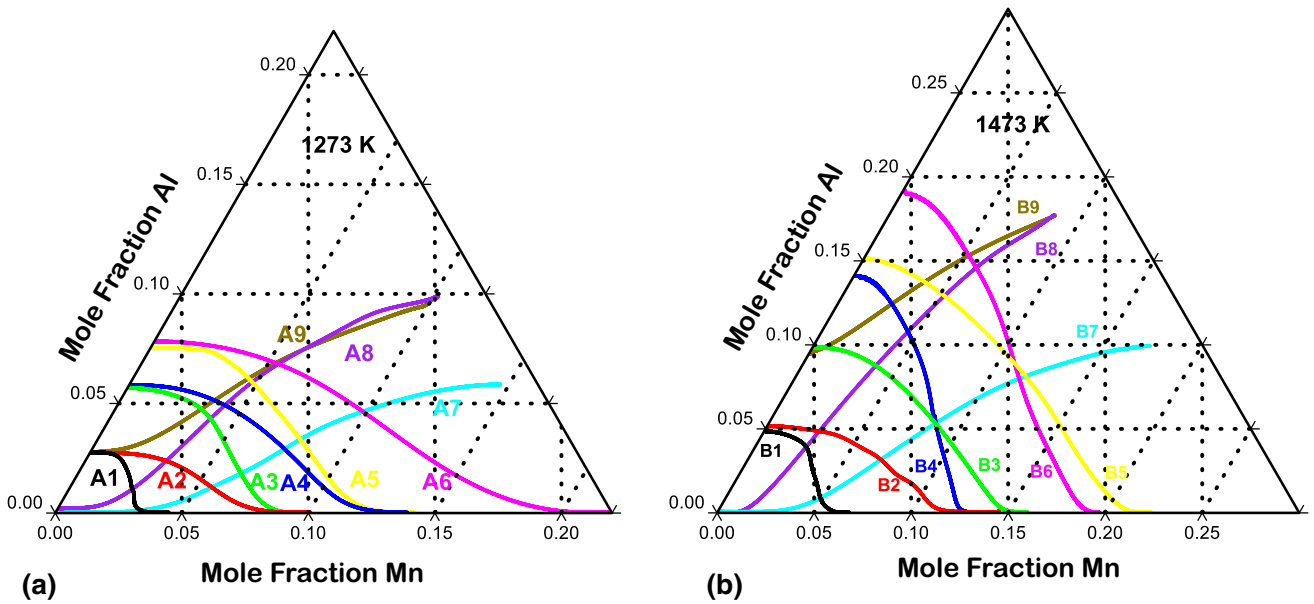

Fig. 2 Diffusion paths for Ti-Al-Mn couples annealed at (a) 1273 K for 50 h, (b) 1473 K for 12 h

Table 3 Interdiffusion coefficients $\tilde{D}_{(\mathrm{Ti-Mn})}$ of BCC Ti-Mn binary alloys (10^{-13} m^2 s^{-1})

at.% Mn	1273 K	1323 K	1373 K	1423 K	1473 K
0	6.01 ± 0.37	8.03 ± 0.45	13.87 ± 0.66	18.95 ± 0.52	23.89 ± 0.34
2	5.94 ± 0.12	8.80 ± 0.08	15.04 ± 0.15	20.46 ± 0.11	33.68 ± 0.12
4	5.73 ± 0.12	8.63 ± 0.08	14.98 ± 0.15	22.14 ± 0.11	36.84 ± 0.12
6	5.52 ± 0.12	8.31 ± 0.08	14.96 ± 0.15	23.88 ± 0.11	39.35 ± 0.12
8	5.33 ± 0.12	8.03 ± 0.08	15.08 ± 0.15	25.96 ± 0.11	41.94 ± 0.12
10	5.19 ± 0.12	7.85 ± 0.08	15.37 ± 0.15	28.21 ± 0.11	44.84 ± 0.12
12	5.10 ± 0.12	7.77 ± 0.08	15.87 ± 0.15	29.77 ± 0.11	48.07 ± 0.12
14	5.07 ± 0.12	7.79 ± 0.08	16.52 ± 0.15		51.41 ± 0.12
16	5.09 ± 0.12	7.61 ± 0.08	16.84 ± 0.15		

Table 4 Interdiffusion coefficients of BCC Ti-Al-Mn ternary alloys at 1273 K

Diffusion couple	Composition, at.%		Interdiffusion coefficients (10^{-13} m^2 s^{-1})			
	Al	Mn	$\tilde{D}^{\mathrm{Ti}}_{\mathrm{AlAl}}$	$\tilde{D}^{\mathrm{Ti}}_{\mathrm{AlMn}}$	$\tilde{D}^{\mathrm{Ti}}_{\mathrm{MnMn}}$	$\tilde{D}^{\mathrm{Ti}}_{\mathrm{MnAl}}$
A7–A1	0.12	3.32	1.07 ± 0.16	0.09 ± 0.06	12.11 ± 0.40	17.11 ± 1.49
A7–A2	1.18	5.60	1.77 ± 0.01	0.46 ± 0.01	9.72 ± 0.14	8.47 ± 0.19
A7–A3	1.81	6.44	2.04 ± 0.04	0.64 ± 0.04	11.39 ± 0.29	6.56 ± 0.36
A7–A4	2.92	7.60	2.13 ± 0.03	0.50 ± 0.03	9.12 ± 0.48	7.23 ± 0.36
A7–A5	3.36	8.00	2.21 ± 0.04	0.67 ± 0.04	10.24 ± 0.34	6.90 ± 0.20
A7–A6	4.63	9.83	3.35 ± 0.08	0.94 ± 0.04	10.77 ± 0.25	12.81 ± 0.27
A8–A1	1.06	2.48	0.89 ± 0.05	0.00 ± 0.06	5.44 ± 0.12	0.12 ± 0.03
A8–A2	2.37	3.19	0.90 ± 0.03	0.00 ± 0.05	4.57 ± 0.09	0.44 ± 0.07
A8–A3	4.22	3.93	1.12 ± 0.12	− 0.31 ± 0.03	4.71 ± 0.11	0.23 ± 0.08
A8–A4	4.89	4.23	1.15 ± 0.06	− 0.18 ± 0.05	3.93 ± 0.09	0.46 ± 0.20
A8–A5	5.99	4.81	1.16 ± 0.06	0.14 ± 0.10	3.66 ± 0.12	0.30 ± 0.07
A8–A6	6.76	5.38	1.40 ± 0.61	0.00 ± 0.28	3.32 ± 0.40	0.19 ± 0.78
A9–A3	4.74	3.40	1.35 ± 0.16	− 0.05 ± 0.09	3.78 ± 0.24	− 0.22 ± 0.14
A9–A4	5.14	3.74	1.42 ± 0.08	− 0.01 ± 0.08	3.74 ± 0.01	− 0.18 ± 0.01
A9–A5	6.14	4.57	1.46 ± 0.08	0.33 ± 0.06	3.47 ± 0.10	0.19 ± 0.17
A9–A6	6.83	5.33	1.83 ± 0.19	0.17 ± 0.07	3.33 ± 0.04	0.23 ± 0.07
Average	3.89	5.12	1.58	0.21	6.46	3.80

one pair of diffusion couples whose diffusion paths intersect at a common composition. Note that a lack of data for the compositional dependence of the molar volume in the Ti-Al-Mn alloys imposes the assumption of a constant molar volume for the diffusion couples examined in this study. Errors introduced by assumption of compositional independent molar volume are considered to be well within the accuracy of diffusion coefficients evaluated by using the *W–G* method.[21, 26]

The impurity diffusion coefficients of Al in Ti-Mn and Mn in Ti-Al binary were calculated based on the ERFEX profiles of the A1–A6, C1–C5 and B1–B6 couples by using the generalized Hall method.[27] The composition profiles were first reformulated to obtain an approximately linear

Table 5 Interdiffusion coefficients of BCC Ti-Al-Mn ternary alloys at 1473 K

Diffusion couple	Composition, at.%		Interdiffusion coefficients (10^{-13} m^2 s^{-1})			
	Al	Mn	$\tilde{D}^{Ti}_{AlAl}$	$\tilde{D}^{Ti}_{AlMn}$	$\tilde{D}^{Ti}_{MnMn}$	$\tilde{D}^{Ti}_{MnAl}$
B7–B1	0.93	4.93	7.17 ± 0.40	− 2.28 ± 0.85	42.82 ± 1.85	5.16 ± 1.43
B7–B2	3.17	6.85	9.48 ± 0.23	0.17 ± 0.15	39.36 ± 0.10	8.34 ± 0.32
B7–B3	5.28	8.60	11.06 ± 0.23	− 0.85 ± 0.29	35.94 ± 0.94	11.58 ± 0.52
B7–B4	5.39	8.70	13.06 ± 0.38	− 2.55 ± 0.61	40.52 ± 1.34	7.54 ± 1.27
B7–B5	8.14	11.80	20.72 ± 0.12	1.57 ± 0.08	40.61 ± 0.09	12.26 ± 0.25
B7–B6	8.26	12.01	20.96 ± 0.99	− 0.01 ± 0.97	43.90 ± 1.22	6.30 ± 1.58
B8–B1	3.95	2.64	8.02 ± 0.11	− 2.28 ± 0.31	31.50 ± 0.76	− 0.79 ± 0.49
B8–B2	4.82	2.90	9.01 ± 0.48	− 1.12 ± 0.56	26.91 ± 1.32	0.04 ± 0.42
B8–B3	8.71	3.90	10.91 ± 0.25	0.17 ± 0.73	22.69 ± 0.20	1.32 ± 0.38
B8–B4	10.73	4.49	13.44 ± 0.35	1.41 ± 0.47	23.86 ± 0.36	1.19 ± 0.24
B8–B5	12.9	5.29	18.93 ± 1.10	4.56 ± 0.89	19.8 ± 1.56	3.26 ± 0.35
B8–B6	14.52	6.14	18.92 ± 0.86	− 0.44 ± 0.59	24.03 ± 0.36	1.41 ± 0.40
B9–B4	12.45	2.80	14.76 ± 0.91	3.99 ± 0.77	19.93 ± 0.46	0.52 ± 0.29
B9–B5	13.76	3.81	19.95 ± 0.95	5.84 ± 0.06	18.02 ± 0.13	2.94 ± 0.46
B9–B6	15.32	5.32	20.64 ± 0.83	2.15 ± 1.16	23.56 ± 0.39	− 2.36 ± 0.07
Average	8.56	6.01	14.47	0.69	30.23	3.91

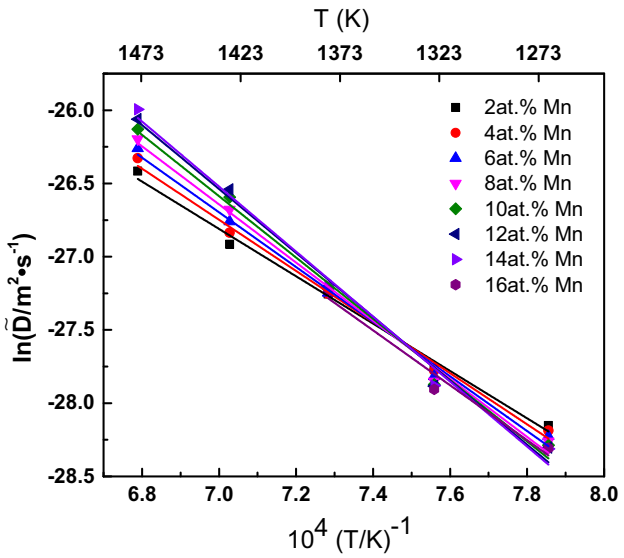

Fig. 4 The Arrhenius plot of the interdiffusion of Ti-Mn binary BCC alloys

plot of $\mu = h\lambda + k$, where $\mu = \mathrm{erf}^{-1}(2Y - 1)$ and $\lambda = x/\sqrt{t}$. The impurity diffusivity of a third element i in binary $j - k$ alloy, i.e. $D^*_{i(j-k)}$ can be evaluated via

$$D^*_{i(j-k)} = \frac{1}{4h^2}\left[1 + \frac{2k}{\sqrt{\pi}}\exp(\mu^2) \times \frac{x_i}{x_0}\right] \quad \text{(Eq 4)}$$

when the limit of $\frac{x_i}{x_0}$ approaches zero at the end of linear range of μ versus λ. In Eq 4 x_i is the composition of i in binary alloys and x_0 represents the composition of i at the other terminal of the diffusion couple.

3 Experimental Results

3.1 Composition Profiles and Diffusion Paths

Figure 1 shows two sets of representative diffusion profiles i.e. the binary couple C5 at 1473 K for 12 h and the ternary couples A4 and A8 at 1273 K for 12 h. Like all other couples, the diffusion zones in these three couples range up to 3 mm with the profiles in typical S-shape. From Fig. 1(b), the penetration depth of Mn element, typical around 3 mm is larger than that of Al element, indicating that the diffusion rate of Mn is faster than that of Al in the BCC Ti-Al-Mn alloys.

Figure 2 shows the diffusion paths of the Ti-Al-Mn ternary couples at 1273 and 1473 K in the ternary isotherms. The paths at both temperatures are clearly bent and S-shaped, once again implying that obvious difference of diffusion rates between Al and Mn.[15] The fact that the ends of all the diffusion paths tend to be along the direction at a constant Al content, i.e. the Ti-Mn vicinity, concludes Al as a slower diffuser.

3.2 Diffusion Coefficients

3.2.1 Ti-Mn Binary

Figure 3 presents the extracted interdiffusion coefficients $\tilde{D}_{Ti-Mn}$ as the function of composition in the temperature ranges from 1273 to 1473 K. The values are listed in Table 3, ranging from 5×10^{-13} to 50×10^{-13} m^2 s^{-1}. It is apparent that the binary interdiffusion coefficients

Table 6 Activation energy Q (kJ mol^{-1}) and pre-exponential factor D_0 ($\times$ 10^{-6} m^2 s^{-1}) of the interdiffusion coefficients of BCC Ti-Mn binary alloys

x_{Mn}/at.%	2	4	6	8	10	12	14
ΔE (kJ mol^{-1})	134.4	145.1	155.2	164.9	174.0	181.4	184.5
D_0 ($\times$ 10^{-6} m^2 s^{-1})	0.186	0.490	1.201	2.882	6.556	12.799	16.892

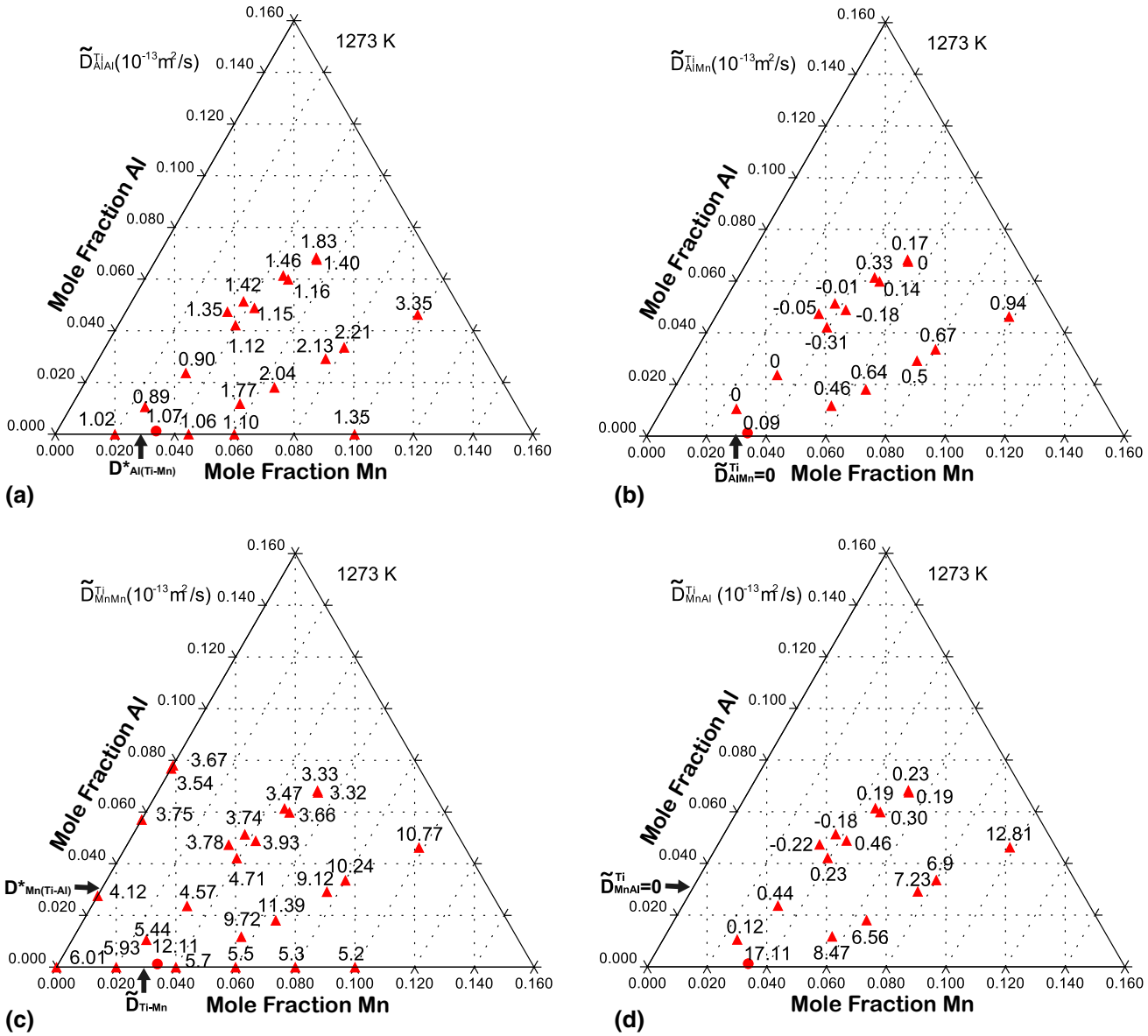

Fig. 5 Main and cross interdiffusion of BCC Ti-Al-Mn ternary alloys, (a) $\tilde{D}^{Ti}_{AlAl}$, (b) $\tilde{D}^{Ti}_{AlMn}$, (c) $\tilde{D}^{Ti}_{MnMn}$ and (d) $\tilde{D}^{Ti}_{MnAl}$ in ternary Ti-Al-Mn alloys at 1273 K

increase with increasing Mn content at 1473 and 1423 K, however, the compositional dependence becomes weakening at lower temperatures 1273-1373 K.

3.2.2 Ti-Al-Mn

The interdiffusion coefficients extracted at the intersection compositions of the diffusion paths are summarized in

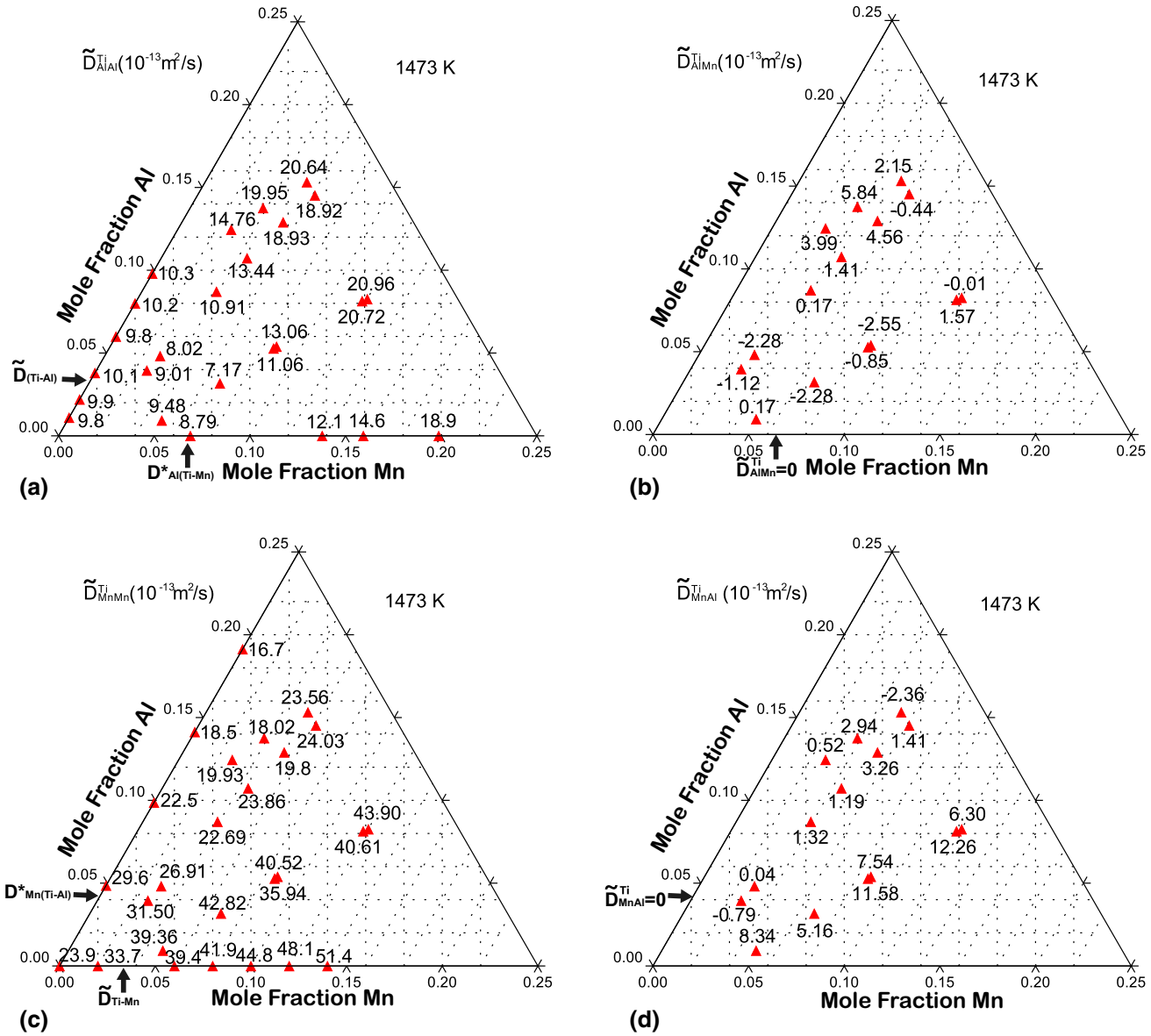

Fig. 6 Main and cross interdiffusion of BCC Ti-Al-Mn ternary alloys, (a) $\tilde{D}^{Ti}_{AlAl}$, (b) $\tilde{D}^{Ti}_{AlMn}$, (c) $\tilde{D}^{Ti}_{MnMn}$ and (d) $\tilde{D}^{Ti}_{MnAl}$ in ternary Ti-Al-Mn alloys at 1473 K

Table 4 for 1273 K and Table 5 for 1473 K. The uncertainty of interdiffusivities was computed by using the standard deviation from multiple measurements of composition profiles.[19, 25] All the main interdiffusion coefficients ($\tilde{D}^{Ti}_{AlAl}$ and $\tilde{D}^{Ti}_{MnMn}$) show positive values and being larger than the cross ones. While some cross terms of $\tilde{D}^{Ti}_{AlMn}$ and $\tilde{D}^{Ti}_{MnAl}$ show negative values, they all are well satisfied with the thermodynamic constraints[28] via

$$\tilde{D}^{Ti}_{AlAl} + \tilde{D}^{Ti}_{MnMn} > 0 \quad \text{(Eq 5a)}$$

$$\tilde{D}^{Ti}_{AlAl} \times \tilde{D}^{Ti}_{MnMn} - \tilde{D}^{Ti}_{AlMn} \times \tilde{D}^{Ti}_{MnAl} \geq 0 \quad \text{(Eq 5b)}$$

$$\left(\tilde{D}^{Ti}_{AlAl} + \tilde{D}^{Ti}_{MnMn}\right)^2 - 4\left(\tilde{D}^{Ti}_{AlAl} \times \tilde{D}^{Ti}_{MnMn} - \tilde{D}^{Ti}_{AlMn} \times \tilde{D}^{Ti}_{MnAl}\right) \geq 0. \quad \text{(Eq 5c)}$$

The average main interdiffusion rate $\overline{\tilde{D}^{Ti}_{MnMn}}$ has the largest values, i.e. 6.46×10^{-13} and 30.23×10^{-13} $m^2\ s^{-1}$ among the four average rates at 1273 and 1473 K, being 4.1, 30.8 and 1.7 times greater than $\overline{\tilde{D}^{Ti}_{AlAl}}$, $\overline{\tilde{D}^{Ti}_{AlMn}}$ and $\overline{\tilde{D}^{Ti}_{MnAl}}$ at 1273 K and 2.1, 43.8 and 7.7 times at 1473 K, respectively.

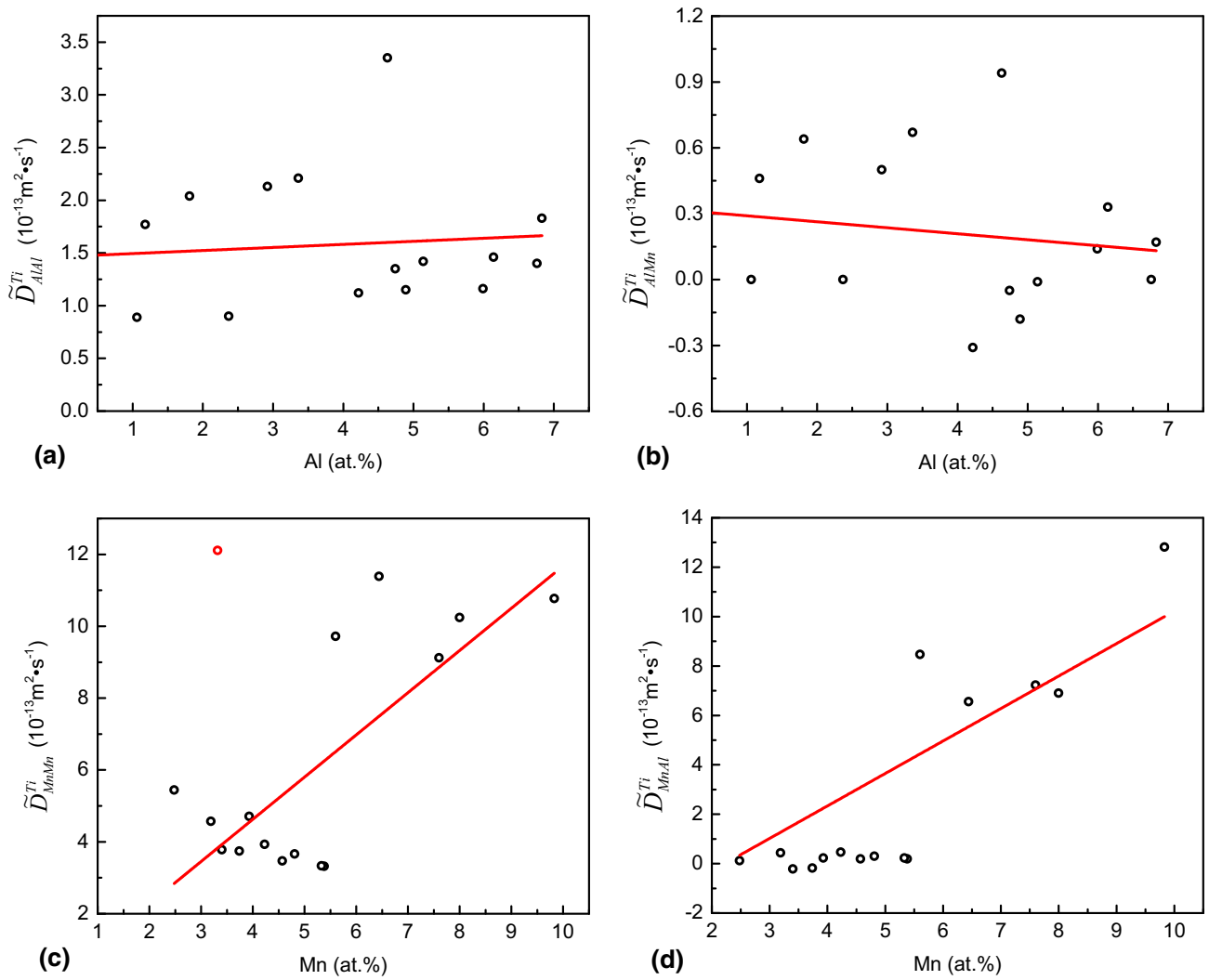

Fig. 7 The variation of ternary interdiffusion coefficients with the composition of diffusing specie at 1273 K, (a) $\tilde{D}^{\mathrm{Ti}}_{\mathrm{AlAl}}$; (b) $\tilde{D}^{\mathrm{Ti}}_{\mathrm{AlMn}}$; (c) $\tilde{D}^{\mathrm{Ti}}_{\mathrm{MnMn}}$; (d) $\tilde{D}^{\mathrm{Ti}}_{\mathrm{MnAl}}$

4 Discussions

4.1 Ti-Mn Binary System

As shown in Fig. 4, the Arrhenius plot is given to describe the temperature dependence of interdiffusion coefficient $\tilde{D}$ of binary Ti-Mn alloys. The liner regression allows the activation energy ΔQ and pre-exponential factor $\tilde{D}_0$ of the binary interdiffusion coefficients to be derived and are listed in Table 6. As it shows, the rise of the Mn content from 2 to 14 at.% leads the change in the activation energy from 134.4 to 184.5 kJ/mol.

4.2 Ti-Al-Mn Ternary System

4.2.1 Interdiffusion Coefficients

The ternary interdiffusion coefficients extracted and listed in Tables 4 and 5 are plotted in Fig. 5 and 6, respectively for 1273 and 1473 K. A rough compositional dependence could be outlined, i.e. at 1273 K, the dependence of all four interdiffusion rates on the Al and Mn contents is weak and ambiguous, nevertheless, the increase of two main coefficients is clearly observed to be with increasing Al or Mn.

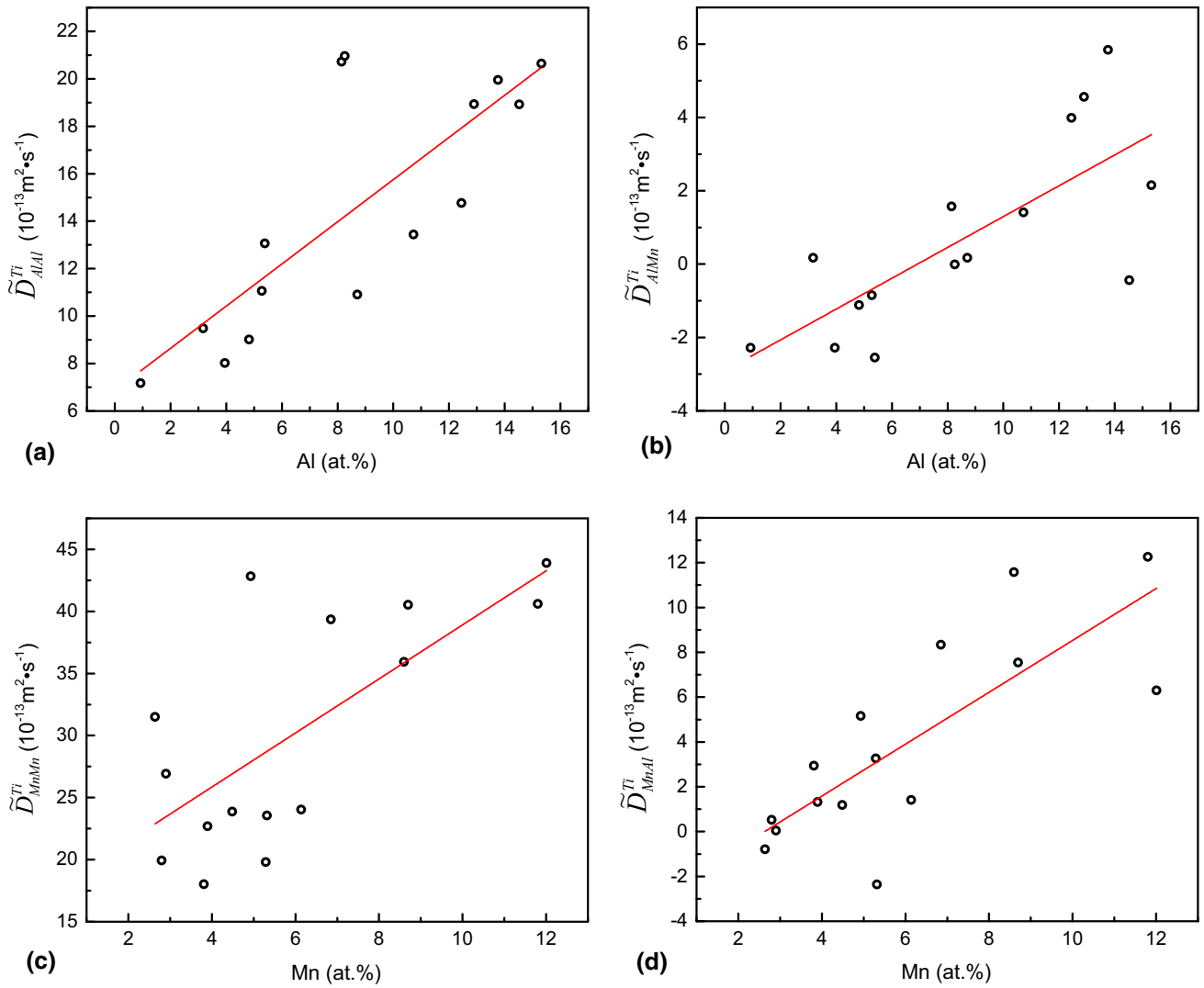

Fig. 8 The variation of ternary interdiffusion coefficients with the composition of diffusing specie at 1473 K, (a) $\tilde{D}^{\mathrm{Ti}}_{\mathrm{AlAl}}$; (b) $\tilde{D}^{\mathrm{Ti}}_{\mathrm{AlMn}}$; (c) $\tilde{D}^{\mathrm{Ti}}_{\mathrm{MnMn}}$; (d) $\tilde{D}^{\mathrm{Ti}}_{\mathrm{MnAl}}$

Table 7 Impurity diffusivities of Al in Ti-Mn and Mn in Ti-Al binary Alloys

Temperature	Composition	Impurity coefficients (m^2/s)	Composition	Impurity coefficients (m^2/s)
1273 K	$D^*_{\mathrm{Al(Ti-4.47Mn)}}$	1.06×10^{-13}	$D^*_{\mathrm{Mn(Ti-2.76Al)}}$	4.12×10^{-13}
	$D^*_{\mathrm{Al(Ti-10.03Mn)}}$	1.35×10^{-13}	$D^*_{\mathrm{Mn(Ti-5.61Al)}}$	3.75×10^{-13}
	$D^*_{\mathrm{Al(Ti-14.11Mn)}}$	1.34×10^{-13}	$D^*_{\mathrm{Mn(Ti-7.69Al)}}$	3.54×10^{-13}
	$D^*_{\mathrm{Al(Ti-21.83Mn)}}$	1.61×10^{-13}	$D^*_{\mathrm{Mn(Ti-7.81Al)}}$	3.67×10^{-13}
1473 K	$D^*_{\mathrm{Al(Ti-6.89Mn)}}$	8.79×10^{-13}	$D^*_{\mathrm{Mn(Ti-4.86Al)}}$	2.96×10^{-12}
	$D^*_{\mathrm{Al(Ti-15.93Mn)}}$	1.46×10^{-12}	$D^*_{\mathrm{Mn(Ti-9.87Al)}}$	2.25×10^{-12}
	$D^*_{\mathrm{Al(Ti-13.78Mn)}}$	1.21×10^{-12}	$D^*_{\mathrm{Mn(Ti-14.13Al)}}$	1.85×10^{-12}
	$D^*_{\mathrm{Al(Ti-19.87Mn)}}$	1.89×10^{-12}	$D^*_{\mathrm{Mn(Ti-19.13Al)}}$	1.67×10^{-12}

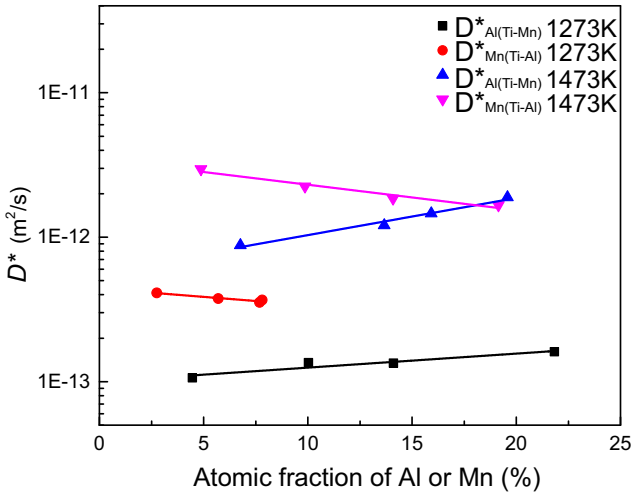

Fig. 9 Impurity diffusivities of Al in Ti-Mn alloys and of Mn in Ti-Al alloys at 1273 K and 1473 K

Table 8 Average main interdiffusion coefficients in Ti-Al-X (Ni, Co, Fe, Mn, Cr, V and Mo) ternary systems at 1473 K

	Average $\tilde{D}^{Ti}_{AlAl}$, m^2/s	Average $\tilde{D}^{Ti}_{XX}$, m^2/s
Ti-Al-Ni	1.9×10^{-12}	2.18×10^{-11}
Ti-Al-Co	1.3×10^{-12}	1.9×10^{-11}
Ti-Al-Fe	1.3×10^{-12}	1.2×10^{-11}
Ti-Al-Mn	1.40×10^{-12}	3.02×10^{-12}
Ti-Al-Cr	7.43×10^{-13}	1.56×10^{-12}
Ti-Al-V	6.8×10^{-13}	4.1×10^{-13}
Ti-Al-Mo	4.5×10^{-13}	1.45×10^{-13}

For a closer look, in Fig. 7 and 8, the variations of ternary interdiffusion coefficients $\tilde{D}^{k}_{ij}$ are re-plotted against the composition of diffusing specie i for 1273 and 1473 K, respectively. At 1273 K, $\tilde{D}^{Ti}_{MnAl}$ and $\tilde{D}^{Ti}_{MnMn}$ are thus noticed to increase with the Mn content whereas $\tilde{D}^{Ti}_{AlAl}$ and $\tilde{D}^{Ti}_{AlMn}$ vary weakly with Al. While at 1473 K, all four ternary interdiffusion coefficients $\tilde{D}^{k}_{ij}$ are unveiled that increase with the increase of composition i, see Fig. 8.

4.2.2 Ternary Impurity Diffusion Coefficient

The impurity diffusivities of Al in Ti-Mn alloys, and Mn in Ti-Al, i.e. $D^{*}_{Al(Ti-Mn)}$ and $D^{*}_{Mn(Ti-Al)}$ were determined by the generalized Hall's method.[27] In Table 7, we summarize the impurity diffusivities of $D^{*}_{Al(Ti-Mn)}$ and $D^{*}_{Mn(Ti-Al)}$, extracted from the A1, A3, A5, A6, B1, B3, B4 and B6 couples. The composition dependence of impurity diffusivities is displayed in Fig. 9. It depicts that $D^{*}_{Al(Ti-Mn)}$ increases with the increase of Mn compositions, while the values of $D^{*}_{Mn(Ti-Al)}$ decrease with the increase of Al composition.

Impurity diffusivities of Al in Ti-Mn ($D^{*}_{Al(Ti-Mn)}$) and Mn in Ti-Al ($D^{*}_{Mn(Ti-Al)}$) together with the binary data of interdiffusion coefficients of Ti-Mn ($\tilde{D}_{(Ti-Mn)}$) and Ti-Al ($\tilde{D}_{(Ti-Al)}$[9]) are also plotted in Fig. 5 and 6. According to Shuck and Toor,[29] the main diffusivities approaching to binary boundary should degenerate to binary inter-diffusivities, i.e.

$$\lim_{C_j \to 0} \tilde{D}^{k}_{ii} = \tilde{D}_{(i-k)}, \quad \text{(Eq 6)}$$

and the cross diffusivities approaching to binary boundary should be asymptotically approaching to zero, i.e.

$$\lim_{C_i \to 0} \tilde{D}^{k}_{ij} = 0. \quad \text{(Eq 7)}$$

The two relations fairly satisfy in Fig. 5 and 6, particularly the good consistency between the binary ($\tilde{D}_{(Ti-Al)}$ and $\tilde{D}_{(Ti-Mn)}$) and ternary interdiffusion and between the impurity ($D^{*}_{Mn(Ti-Al)}$ *and* $D^{*}_{Al(Ti-Mn)}$) and ternary interdiffusion at 1473 K.

4.2.3 Ti-Al-X Ternaries

A systematic comparison of the average main interdiffusion coefficients at 1473 K in seven Ti-Al-X (Ni,[14] Co,[19] Fe,[13] Mn, Cr,[30] V,[31] Mo[15]) ternary systems is presented in Table 8. The Mn main rate is one order magnitude smaller than that of Ni, Co and Fe while two times greater than Cr and one order magnitude greater than V and Mo, revealing that the order of the average main interdiffusion coefficients $\overline{\tilde{D}^{Ti}_{XX}}$ (X = Ni, Co, Fe, Mn, Cr, V and Mo) exhibits $D_{Ni} > D_{Co} > D_{Fe} > D_{Mn} > D_{Cr} > D_{V-} > D_{Mo}$. It is reported that the diffusion of Ni, Co and Fe in β-Ti is predominantly of interstitial nature (or occurring by a mixed mechanism[12, 14, 31, 32]), and the presence of these elements likely enhances the Al diffusion as well. The diffusion in Ti-Al-(Cr, V and Mo) obeys a normal vacancy mechanism. The element Mn is in between, so that the diffusion mechanism of Mn in Ti-Al-Mn should be the mixed mechanism of the two.

5 Conclusions

In summary, the interdiffusion in bcc Ti-Mn binary and Ti-Al-Mn ternary alloys was investigated between 1273 and 1473 K. The inter- and impurity diffusivities were extracted and are summarized as follows:

1. Interdiffusion diffusion coefficients of BCC Ti-Mn binary alloys extracted by the *S–F* method at the temperature range from 1273 to 1473 K. The binary

interdiffusion coefficients increase with increasing Mn content.

2. The ternary inter- and impurity diffusivities were extracted by *W–G* and generalized Hall methods, respectively. It was demonstrated that, all four diffusion coefficients $\tilde{D}_{ij}^{k}$ (i, j = Al, Mn), both main and cross ones, increase with increasing the composition of diffusing specie at 1473 K, whereas at 1273 K $\tilde{D}_{\mathrm{MnMn}}^{\mathrm{Ti}}$ and $\tilde{D}_{\mathrm{MnAl}}^{\mathrm{Ti}}$ are enhanced by the addition of diffusing specie Mn but $\tilde{D}_{\mathrm{AlAl}}^{\mathrm{Ti}}$ and $\tilde{D}_{\mathrm{AlMn}}^{\mathrm{Ti}}$ are in weak dependence with the Al content.
3. A complete comparison among seven Ti-Al-X (Ni, Co, Fe, Mn, Cr, V and Mo) ternary systems reveals that the order of the average main interdiffusion coefficients $\overline{\tilde{D}_{\mathrm{XX}}^{\mathrm{Ti}}}$ (X = Ni, Co, Fe, Mn, Cr, V and Mo) exhibits $D_{\mathrm{Ni}} > D_{\mathrm{Co}} > D_{\mathrm{Fe}} > D_{\mathrm{Mn}} > D_{\mathrm{Cr}} > D_{\mathrm{V}} > D_{\mathrm{Mo}}$.

Acknowledgments This work is supported by the National Natural Science Foundation of China (No. 51571113) and Joint Project of Industry-University-Research of Jiangsu Province (Grant No: BY2016005-02). YG would like to thank the support from the National Natural Science Foundation of China (No. 11647162) and Priority Academic Program Development of Jiangsu Higher Education Institution (PAPD). GX wishes to gratefully acknowledge the financial support by the National Natural Science Foundation of China (No. 51701094) and the Natural Science Foundation of Jiangsu Province (BK20171014).

References

1. R.R. Boyer, Attributes, Characteristics, and Applications of Titanium and Its Alloys, *JOM*, 2010, **62**(5), p 21-24
2. O.M. Ivasishin, P.E. Markovsky, Y.V. Matviychuk, S.L. Semiatin, C.H. Ward, and S. Fox, A Comparative Study of the Mechanical Properties of High-Strength *β*-Titanium Alloys, *J. Alloys Compd.*, 2008, **457**(1), p 296-309
3. G. Lütjering and J.C. Williams, *Titanium*, Springer, Berlin, 2007
4. A.V. Mikhaylovskaya, A. Omar, A.D. Kotov, J.S. Kwame, T. Pourcelot, I.S. Golovin, and V.K. Portnoy, Superplastic Deformation Behaviour and Microstructure Evolution of Near-α Ti-Al-Mn Alloy, *Mater. Sci. Eng. A*, 2017, **708**, p 469-477
5. Y. Sumi, S. Ueta, M. Ueda, and M. Ikeda, Mechanical Properties of Ti-Mn-Al-Fe Alloys After Solution Heat Treatment, *Mater. Sci. Forum*, 2014, **783–786**, p 597-601
6. J.W. Lu, P. Ge, and Y.Q. Zhao, Recent Development of Effect Mechanism of Alloying Elements in Titanium Alloy Design, *Rare Metal Mater. Eng.*, 2014, **43**(4), p 0775-0779
7. L. Feng, J.S. Li, L. Huang, H. Chang, Y.W. Cui, and L. Zhou, Interdiffusion Behavior of Ti-Mo Binary System in *β* Phase, *Chin. J. Nonferrous Metals*, 2009, **19**(10), p 1766-1771
8. A. Laik, G.B. Kale, and K. Bhanumurthy, Interdiffusion Studies between a Mo-Based Alloy and Ti, *Metall. Mater. Trans. A*, 2006, **37A**(10), p 2919-2926
9. S.Y. Lee, O. Taguchi, and Y. Iijima, Diffusion of Aluminium in *β*-Titanium, *Mater. Trans.*, 2010, **51**(10), p 1809-1813
10. I. Thibon, D. Ansel, and T. Gloriant, Interdiffusion in *β*-Ti-Zr Binary Alloys, *J. Alloys Compd.*, 2009, **470**(1–2), p 127-133
11. C.P. Wang, Y.S. Luo, Y. Lu, J.J. Han, Z. Shi, Y.H. Guo, and X.J. Liu, Interdiffusion and Atomic Mobilities in BCC Ti-Ga and Ti-Cu Alloys, *J. Phase Equilib. Diffus.*, 2017, **38**(2), p 84-93
12. T. Takahashi, Ternary Diffusion and Thermodynamic Interaction in the *β* Solid Solutions of Ti-Al-Co Alloys, *J. Jpn. Inst. Metals*, 2009, **59**(8), p 432-438
13. T. Takahashi and Y. Minamino, Ternary Diffusion and Thermodynamic Interaction in the *β* Solid Solutions of Ti-Al-Fe Alloys at 1423 K, *J. Alloys Compd.*, 2012, **545**, p 168-175
14. B. Gao, Y.Y. Gu, Q.J. Wu, Y.H. Guo, and Y.W. Cui, Diffusion Research in BCC Ti-Al-Ni Ternary Alloys, *J. Phase Equilib. Diffus.*, 2017, **38**(4), p 502-508
15. Y. Chen, B. Tang, G.L. Xu, C.Y. Wang, H.C. Kou, J.S. Li, and Y.W. Cui, Diffusion Research in BCC Ti-Al-Mo Ternary Alloys, *Metall. Mater. Trans. A*, 2014, **45A**(4), p 1647-1652
16. E. Santos and F. Dyment, Solvent and Solute Diffusion in B.C.C. Ti-Co and Ti-Mn Alloys, *Philos. Mag.*, 1975, **31**(4), p 809-827
17. Y. Nakamura, H. Nakajima, S. Ishioka, and M. Koiwa, Effect of Oxygen on Diffusion of Manganese in α Titanium, *Acta Metall.*, 1988, **36**(10), p 2787-2795
18. L.Y. Chen, C.H. Li, A.T. Qiu, X.G. Lu, W.Z. Ding, and Q.D. Zhong, Calculation of Phase Equilibria in Ti-Al-Mn Ternary System Involving a New Ternary Intermetallic Compound, *Intermetallics*, 2010, **18**(11), p 2229-2237
19. Y. Chen, J.S. Li, B. Tang, G.L. Xu, H.C. Kou, and Y.W. Cui, Interdiffusion in FCC Co-Al-Ti Ternary Alloys, *J. Phase Equilib. Diffus.*, 2015, **36**(2), p 127-135
20. F. Sauer and V. Freise, Diffusion in Binären Gemischen Mit Volumenänderung, *Z. Elektrochem. Ber. Bunsenges. Phys. Chem.*, 1962, **66**(4), p 353-362
21. D.P. Whittle and A. Green, The Measurement of Diffusion Coefficients in Ternary Systems, *Scr. Mater.*, 1974, **8**(7), p 883-884
22. T. Ahmed, I.V. Belova, and G.E. Murch, Finite Difference Solution of the Diffusion Equation and Calculation of the Interdiffusion Coefficient Using the Sauer–Freise and Hall Methods in Binary Systems, *Procedia Eng.*, 2015, **105**(247), p 570-575
23. J.S. Kirkaldy, Diffusion in Multicomponent Metallic Systems, *Can. J. Phys.*, 1957, **35**(4), p 435-440
24. F.J.A. den Broeder, A General Simplification and Improvement of the Matano–Boltzmann Method in the Determination of the Interdiffusion Coefficients in Binary Systems, *Scr. Mater.*, 1969, **3**(5), p 321-325
25. C.Y. Wang, G.L. Xu, and Y.W. Cui, Mapping of Diffusion and Nanohardness Properties of Fcc Co-Al-V Alloys Using Ternary Diffusion Couples, *Metall. Trans. A*, 2017, **48**(9), p 1-11
26. J.A. Nesbitts and R.W. Heckel, Interdiffusion in Ni-Rich, Ni-Cr-Al Alloys at 1100 and 1200 °C: part II. Diffusion Coefficients and Predicted Concentration Profiles, *Metall. Trans. A*, 1987, **18**, p 2075-2086
27. L.D. Hall, An Analytical Method of Calculating Variable Diffusion Coefficients, *J. Chem. Phys.*, 1953, **21**, p 87-89
28. J.S. Kirkaldy, D. Weichert, and Z. Ul Haq, Diffusion in Multicomponent Metallic Systems: VI. Some Thermodynamic Properties of the D Matrix and the Corresponding Solutions of the Diffusion Equations, *Can. J. Phys.*, 1963, **41**(12), p 2166-2173
29. F.O. Shuck and H.L. Toor, Diffusion in the Three Component Liquid System Methyl Alcohol-*n*-Propyl Alcohol-Isobutyl Alcohol, *J. Phys. Chem.*, 1963, **67**(3), p 540-545
30. T. Takahashi, N. Matsuda, S. Kubo, T. Hino, M. Komatsu, and K. Hisayuki, Interdiffusion in the *β* Solid Solution of Ti-Al-Cr System, *J. Jpn. Inst. Metals*, 2004, **54**(7), p 280-286
31. T. Takahashi, Y. Minamino, and M. Komatsu, Interdiffusion in *β* Phase of the Ternary Ti-Al-V System, *Mater. Trans.*, 2008, **49**(1), p 125-132
32. G.M. Hood and R.J. Schultz, Ultra-fast Solute Diffusion in α-Ti and α-Zr, *Philos. Mag.*, 1972, **26**(2), p 329-336